

KMTNet Photometry

Yuan Qi Ni

January 1, 2018

Abstract

This document describes the current iteration of the KMTNet Photometry routines. Capabilities include PSF photometry, aperture photometry, image subtraction, noise estimation, and limiting magnitude estimation. Included are detailed descriptions of current implementation, as well as some tests on KMTNet data to establish some behavioral benchmarks.

1 Introduction

The routines described in the following document were written with the purpose of analyzing astronomical data in the form of fits images. Several goals were established early on in the project. These goals include PSF photometry for bright sources, simple aperture photometry for faint sources that may not have an easily extracted PSF, image subtraction, and photometry on differenced images. After many iterations we've arrived at temporary solutions. These solutions are probably not optimal, but their behaviour falls within tolerance of our expectations. Some of these expectations include correct measurements of known magnitudes, and proper relationship between intensity and noise under PSFs.

In section 2, we describe components of the current iteration of the KMTNet Photometry routines available on the git repository at <https://github.com/niyuan1/SNAP>. In section 3, we use a sample dataset to show that behavior over a wide operating range conforms with expectations, and establish some performance benchmarks. In section 4, we give some concluding remarks about where the software may be made more optimal.

2 Implementation

The following behaviors are achieved by the current implementation:

1. Extracting average PSF from a set of reference stars.
2. Fitting extracted PSF to stars and integrating using analytic expression.
3. Using extracted PSF to define Kron aperture in which to integrate by direct summation.
4. Using given radius to perform simple aperture photometry.

5. Fitting planar sky background to annulus around sources so that more sophisticated background subtraction can be applied before PSF fitting or aperture integration.
6. Using given list of reference stars to calibrate photometric magnitudes. Can also query AAVSO catalog for lists of reference stars.
7. Using HOTPANTS [1] to subtract reference image from science image and performing photometry on difference science image.
8. Measuring limiting magnitude at given location

2.1 PSF photometry

Point spread function, or image kernel, is the characteristic distribution measured by a detector of a source of photons best approximated by a dimensionless point. An ideal image with perfect resolution would render all point sources as direct delta distributions. However, even in ideal scenarios diffraction limits the resolution of images, and the PSF is described by an Airy disk. KMTNet image resolution is limited by atmospheric turbulence, and PSFs in this regime are best approximated by Moffat functions.

Routine currently approximates PSF using an elliptical moffat distribution described by equation 1. It is characterized by 4 parameters: x, y semi major axes (a_x , a_y), sharpness β , and orientation angle θ .

$$f(x, y) = \frac{\beta - 1}{\pi a_x a_y} \left(1 + \left(\frac{x \cos \theta + y \sin \theta}{a_x} \right)^2 + \left(\frac{y \cos \theta - x \sin \theta}{a_y} \right)^2 \right)^{-\beta} \quad (1)$$

Any particular point source is approximated by 7 parameters in an analytic point source function: central position and amplitude, in addition to 4 parameters describing PSF shape. Fit is performed in an aperture of size $3M$ around the source, where M is a given upper bound on the size of full-width half maxima in an image (usually $M = 5$). Fit χ^2/dof scores between 0.5 and 2.0 consistently for most stable reference stars in KMTNet images. Routine extracts the 4 parameter PSF shape of a given region by fitting 7 parameter PSF to various reference stars in some region and taking weighted average shape using fit parameter errors. Scipy leastsq is used for fitting, which performs nonlinear optimization using gradient descent and returns fit parameters as well as parameter errors.

Routine also implements planar background subtraction before fitting point sources. Here planar background is approximated by the 3 parameter function in Equation 2. Background fit is performed in an annulus around each source. Annulus will be chosen to be either $4M$ - $5M$ in radius or $6M$ - $7M$ where larger annuli are preferred (to minimize source light). However, larger annuli also have higher possibility of containing other bright sources. Hence the annulus whose mean intensity is smallest is always chosen. In this annulus is also where background noise around a source is measured. Standard deviation of the residuals of planar fit to annulus is taken as noise

in background, which includes atmospheric turbulence and read noise.

$$s(x, y) = ax + by + c \quad (2)$$

PSF Photometry: PSF is extracted from reference stars, global PSF shape is fitted to source object and reference stars, point sources are integrated analytically, and source magnitude is calibrated with respect to reference star catalog magnitudes. Integration is purely analytic and hence measured intensity relies completely on the quality of the PSF fit. Error in measured intensity is estimated by adding contributions from Poisson noise and background noise in Equation 3. Here aperture size is taken to be the size in pixels of the elliptical aperture which contains 90% of source light (Kron aperture) which is analytically calculated for the Moffat function.

$$\delta I_{obj} = \sqrt{I_{obj} + (Noise * Size) * 2} \quad (3)$$

Calibration of measured intensity with respect to the i^{th} reference star follows Equation 4, where F_0 is the flux zero point of the filter used to take the image in Janskies. Error in this calibration is given in Equation 5. Notice that δI_{obj} is not a random error among calibrations with respect to different reference stars, but shared amongst all and is not included in $\delta F_{ref,i}$.

$$F_{obj,i} = F_0 \frac{I_{obj}}{I_{ref,i}} 10^{-M_{ref,i}/2.512} \quad (4)$$

$$\delta F_{ref,i} = F_{obj,i} \sqrt{\left(\frac{\delta I_{ref,i}}{I_{ref,i}}\right)^2 + \left(\frac{\ln(10)}{2.512} \delta M_{ref,i}\right)^2} \quad (5)$$

Calibrated flux of source is calculated with respect to each i^{th} reference star using Equation 4. We take a weighted mean of those to get the measured flux of the source F_{obj} . Error of weighted mean δF_{ref} is a random error term due to the variance among reference stars. Total error in measured flux of the source is the sum in quadrature of noise under the source and this random error term due to reference stars. Noise under the source, denoted F_{src} , contributes error calculated by Equation 6, where signal to noise is an invariant quantity. We can then calculate total error in measured flux by Equation 7. Fluxes in Janskies are easily converted to apparent magnitudes.

$$\delta F_{src} = F_{obj} \frac{\delta I_{obj}}{I_{obj}} \quad (6)$$

$$\delta F_{obj} = \sqrt{(\delta F_{src})^2 + (\delta F_{ref})^2} \quad (7)$$

Note that PSF fit residual does not constitute any measurement error in calibrated flux. δF_{obj} constitutes only random errors and does not account for any systematics. Moreover, so long as the objects we are concerned with are measured with the same global PSF function, there should be no systematic error. That is because under the assumption that all point sources in a region of the image have the same PSF shape, the PSF fit to each point source deviates from the real shape in a scale invariant way. Integration of the best fit approximation always falls short of the actual PSF by some constant factor that cancels out in Equation 4 when intensities are divided.

2.2 Aperture photometry

Aperture photometry may be selected over PSF photometry. Aperture photometry can be a better choice than PSF photometry for very faint sources with ill-defined PSF. For the construction of very early light curves, it is better to use aperture photometry for more robust measurements. It is also more robust in general, since no matter what happens to a source, it is always possible to manually integrate pixels. However, that means it is not always the most reliable. When point sources are contaminated by cosmic rays, image subtraction artifacts, or any contamination that can't be eliminated by planar background subtraction, aperture photometry will add all light indiscriminately. PSF photometry on the other is more robust to disturbances in PSF shape, since shape is constrained to be moffat function.

Aperture photometry is set by choice of aperture radius. The same circular aperture is applied globally across the image to the source and to all reference stars. After planar background subtraction, intensity is measured by direct summation of pixels in aperture. Intensities are calibrated in the same way as described in Section 2.1. Aperture may be manually selected by user, or may be set by image PSF. The second method extracts PSFs from standard reference stars as in Section 2.1, and uses the analytic PSF shape to determine a Kron aperture. This is an elliptical aperture containing 90% of source light, and can be determined for the moffat function. The average of semi-major axes for this Kron aperture defines a Kron radius. Routine then applies Kron aperture globally to integrate intensities.

2.3 Image Subtraction

Image subtraction is performed using HOTPANTS [1], which seeks to photometrically match science image with reference image by finding the image kernels and performing convolution. Photometrically matched images may be scaled and subtracted. Result is a differenced science image where stable unsaturated sources present in the reference image have been subtracted almost completely. HOTPANTS uses an analytic kernel composed of a number of gaussian distributions. Consequence of using kernel to perform photometric matching, saturated sources wont convolve in the right way because of saturation artifacts and hence will leave significant residuals. Images are also divided into discrete regions in which photometric matching and subtraction is done separately. Hence some artifacts also remain along the boundaries after subtraction.

It worth noting that the PSF of the source in the subtracted images is significantly different from reference stars in the science image, leading to incorrect photometry on the subtracted image based on the measured PSF from reference stars of the science image. To avoid this error, we can output a modified science image with a matched PSF on HOTPANTS. This modified science image is essentially the convolution of the science image with the kernel. This way the PSF is measured on the modified science image and the photometry is done on the subtracted image.

2.4 Limiting Magnitude

Limiting magnitude is the magnitude of the dimmest star detectable at some image location. Here, detectable means above the signal to noise threshold (typically 2 or 3) required for detection at a given confidence. We find limiting magnitude by evaluating magnitudes of stars synthesized using the measured image point spread function, where we are allowed to vary the height alone. We generate 10 sources of various brightnesses and we evaluate their intensities using their analytic expression. We use measured noise at the image location to evaluate what the signal to noise ratio would be for each synthetic source. Taking the two synthetic sources that are closest to the detection threshold (above and below), we take a finer brightness binning between the two and evaluate again. If all sources are above or below the required signal to noise ratio, we relax the upper or lower bound of the binning by an order of magnitude. In this way, we are able to converge to the detection threshold within a few iterations.

3 Behavior

I will use the N5128-1.Q1.SN dataset as prototype to establish the following behaviours:

1. Extracted PSFs are good approximations to bright point sources
2. Kron apertures nearly optimize signal to noise ratio in aperture photometry
3. Measured magnitudes of reference stars, of widely varying brightness, should match those given in the catalog.
4. Measured magnitudes using the PSF photometry and Aperture photometry methods should match each other for standard reference stars.
5. Noise and Intensity should have the proper scaling relation.
6. Image subtraction should remove all stable stars, with possible exception of saturated stars where residuals may remain.
7. Measured magnitudes before and after subtraction should match if there is no host galaxy.

3.1 PSF extraction

To test PSF extraction (Point 1), I chose an image whose limiting magnitude is 21.9 mags. Then I took a range of 1409 reference stars with magnitudes from 14.0 (prevent saturation) to 17.5 mags. Figure 1 is extracted PSF for a typical reference star in that range. A typical measure of fit quality is the parameter χ^2/dof , where $\chi^2/dof \gg 1$ is characteristic of underfit, and $\chi^2/dof \ll 1$ is characteristic of overfit. Figure 2 is a histogram of all reference stars over their PSF extraction fit χ^2/dof . We can see that median χ^2/dof is on order 1. Hence 7 parameter Moffat fit fits reference stars quite well.

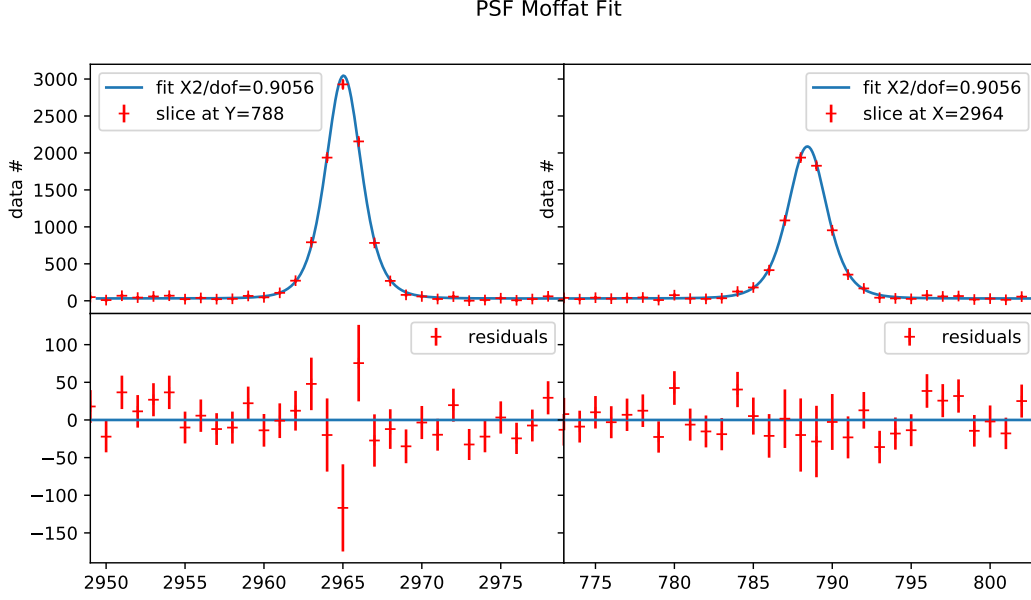


Figure 1: Extracted PSF of a 17.2 mag reference star in B band.

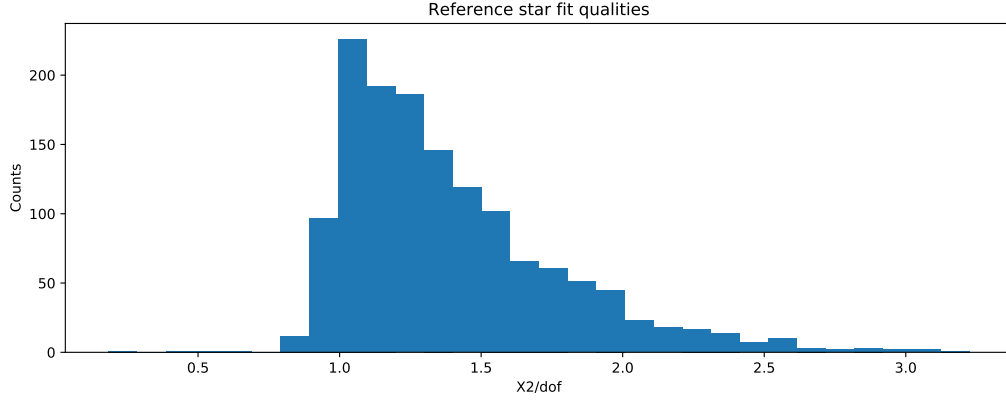


Figure 2: Histogram of reference stars over their PSF extraction fit χ^2/dof .

3.2 Aperture selection

Aperture photometry is in essence an optimization problem for the radius that can extract the maximum signal to noise from a source. Selecting too small of an aperture will miss valuable source light at the wings and hence decrease signal to noise ratio. Selecting too large an aperture will incorporate a lot of pixels in which signal is weaker than noise and hence decrease signal to noise ratio. The optimal aperture incorporates source light up to where the signal to noise tradeoff of adding an extra pixel is no longer justifiable. The Kron aperture containing 90% of source light for a point source contains nearly the optimal amount of light. We aperture photometry for the same reference star whose PSF is shown in Figure 1 using a variety of PSFs. In Figure 3 we plot intensity as well as signal to noise ratio in aperture as a function of aperture radius. Green

line shows the Kron aperture radius. We can see that it incorporates $\sim 90\%$ of total intensity and almost captures the optimal signal to noise ratio (Point 2).

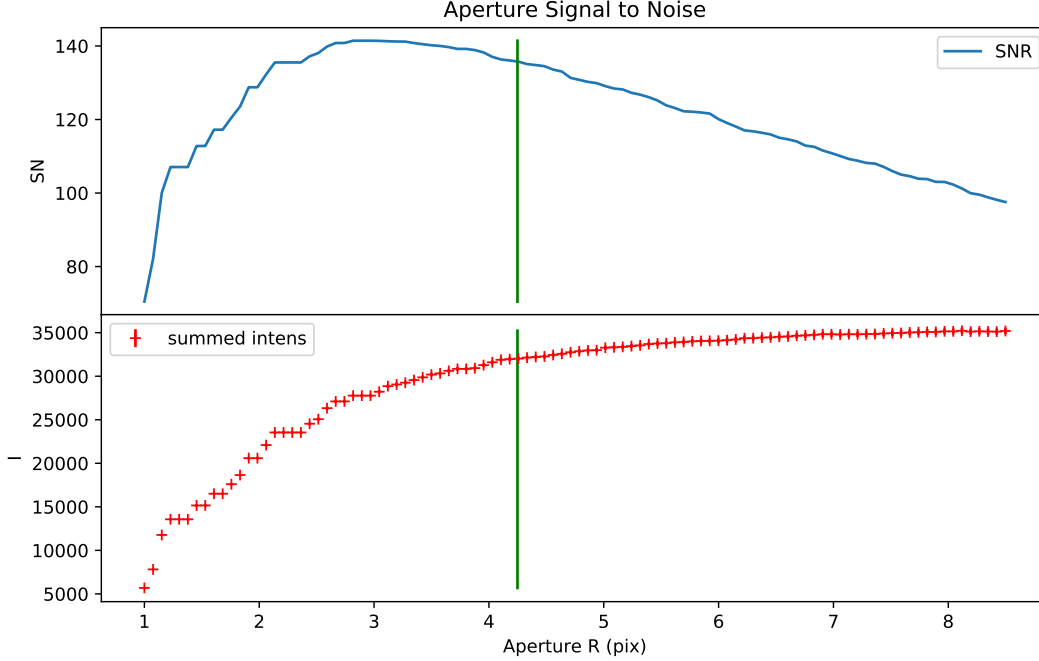


Figure 3: Aperture photometry of a 17.2 mag reference star in B band over a range of apertures. Green vertical line is Kron aperture radius.

3.3 Magnitude Measurement

To test magnitude measurement (Points 3, 4), I chose again the image whose limiting magnitude is 21.9 mags. Then I took a range of 1409 reference stars with magnitudes from 14.0 (prevent saturation) to 17.5 mags. Figure 4 plots measured magnitudes by aperture and PSF photometry against catalog magnitudes. Blue solid line indicates photometric solution. Fit bias is low, though variance is quite high. Assuming catalog magnitudes and errors are closer to reality than our own, our errorbars seem to be consistently underestimated and incommensurate with our high variance.

3.4 Noise Measurements

To test noise intensity relation (Point 5), I chose again the image whose limiting magnitude is 21.9 mags. Then I took a range of 1409 reference stars with magnitudes from 14.0 (prevent saturation) to 17.5 mags. This should be sufficient to probe the high intensity regime (where noise is Poissonian) as well as the low intensity regime (where noise is background dominated). Figure 5 is a log scale plot of measured noise vs intensity (catalog magnitudes) of the reference stars. The red scattered points are measured noise of various reference stars. At high intensity,

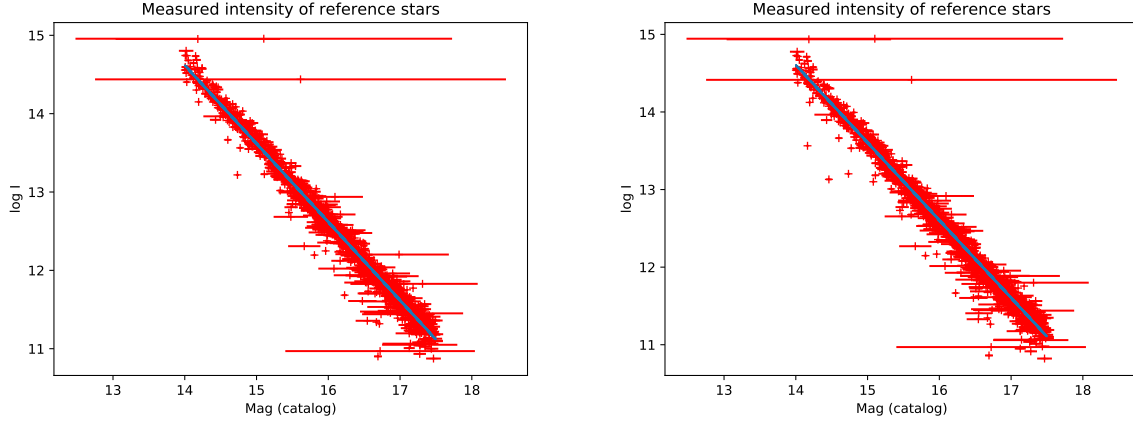


Figure 4: Comparison of calculated magnitudes to catalog magnitudes. (left) Calculated using aperture photometry. (right) Calculated using PSF photometry.

we can see that slope is similar to the blue solid line, which has slope of $-1/2$, consistent with prediction of photon dominated noise. At lower intensities we can see the characteristic taper where noise becomes flat as we approach background dominated noise. This behavior is apparent for both aperture and PSF photometry.

3.5 Image Subtraction

To test efficacy of image subtraction (Points 6, 7), we use a coadded reference image, and 26 science images taken approximately one year later of the same sky. The science images contain a bright unsaturated source of varying brightness, not present to deep limits in the reference image.

As a basic test, we subtracted reference image from itself, expecting the residuals to contain noise only. The result is displayed in Figure 6 (left). Note background noise standard deviation in reference image is ~ 4.0 , so the subtraction is almost complete. Some trends in residuals may be seen where the the image has been divided into 4 quadrants before subtraction. As a second basic test, we subtracted the reference image from a single science image. The result is displayed in Figure 6 (right). Subtraction of saturated stars invariably leaves bright residuals, but subtraction of any unsaturated stable sources leaves almost none.

To test efficacy of photometry routines on subtracted images, we first measure magnitude of transient source in original science images. After subtraction of reference image from each science image, we apply photometry on subtracted images. In Figure 7, we plot measured magnitude of transient source in subtracted vs original image for both aperture and PSF photometry. Magnitudes measured before and after subtraction agree within error, with PSF photometry performing slightly better. This is probably due to its ability to isolate PSF shape from subtraction artifacts.

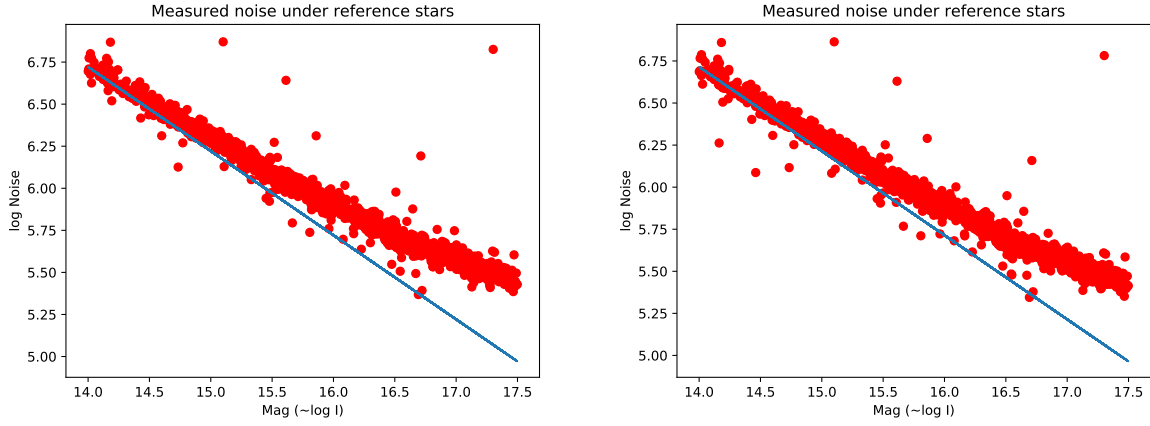


Figure 5: Plot of measured noise vs measured intensity. We can see that for bright stars, noise scales with the square root of intensity in the Poissonian regime, whereas for dim stars noise flattens out in the background dominated regime. (left) Calculated using aperture photometry. (right) Calculated using PSF photometry.

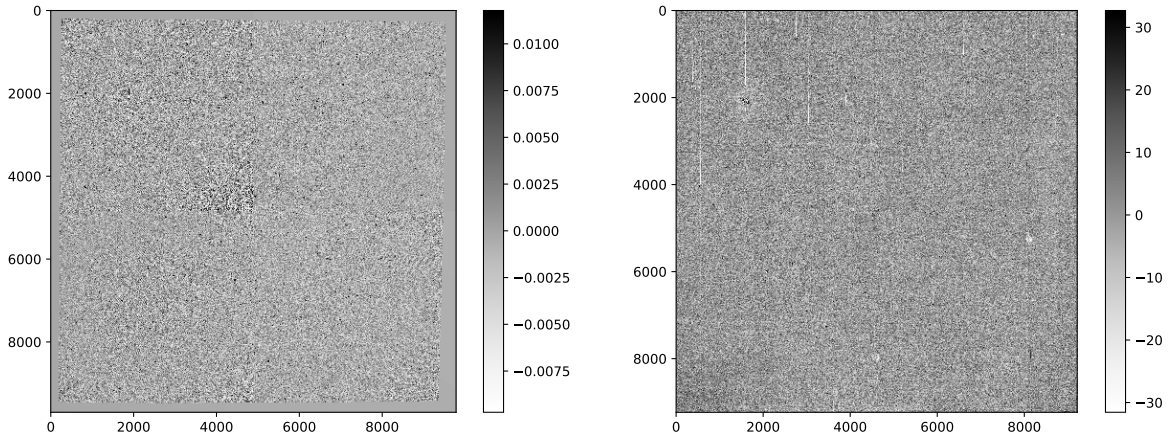


Figure 6: (left) Subtracted reference image from reference image. (right) Subtracted reference image from science image taken of the same sky one year later.

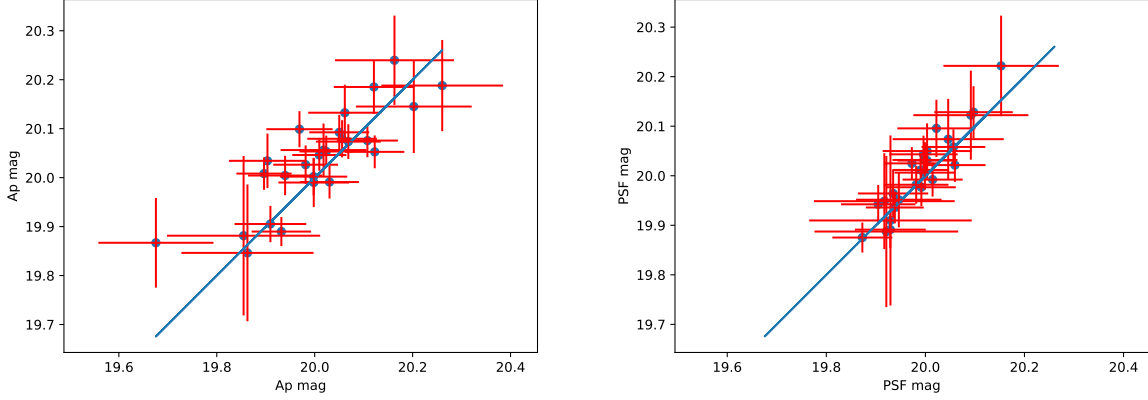


Figure 7: Comparison of calculated magnitudes of a single source in several images before vs after image subtraction. Images is uncrowded with no host galaxy. (left) Calculated using aperture photometry. (right) Calculated using PSF photometry.

4 Conclusion

In the current iteration of KMTNet photometry, routines are capable of performing their functions within tolerable confidence. Several improvements come to mind for future implementations that will greatly optimize performance of KMTNet photometry.

1. Analytic moffat function may be a reasonably good approximation to PSF shape, but Scipy fitting algorithms deal with issues of convergence and proper error estimation. Implementing some kind of bayesian parameter estimation software like Emcee [2] will have more meaningful error estimation.
2. Currently aperture photometry performs simple summation of background subtracted apertures. However, future implementation of software to clean hot pixels or cosmic rays would be much more robust.
3. Image subtraction with HOTPANTS is slightly outdated. Current state of the art image subtraction seems to be using Zackay, Ofek, and Gal-Yam's optimal image subtraction algorithm [3]. In the future, it will better to use an existing implementation or even implement this ourselves for image subtraction.
4. Currently routines are all single threaded, though many parts can easily be made multi-threaded such as PSF extraction. This is because the routines are intended to be used for constructing light curves, in which case it is up to the user to multithread processing of each individual image. More routines will be written to automate the process of light curve generation from a database of images.

References

- [1] A. Becker, “HOTPANTS: High Order Transform of PSF ANd Template Subtraction.” Astrophysics source code library, Apr., 2015.
- [2] D. Foreman-Mackey, D. W. Hogg, D. Lang, and J. Goodman, “emcee: The MCMC Hammer,” **125** (Mar., 2013) 306, [arXiv:1202.3665](#) [[astro-ph.IM](#)].
- [3] B. Zackay, E. O. Ofek, and A. Gal-Yam, “Proper Image SubtractionOptimal Transient Detection, Photometry, and Hypothesis Testing,” **830** (Oct., 2016) 27, [arXiv:1601.02655](#) [[astro-ph.IM](#)].